NANO LETTERS

LETTER

pubs.acs.org/NanoLett

Robust, Functional Nanocrystal Solids by Infilling with Atomic Layer Deposition

Yao Liu,[†,‡] Markelle Gibbs,[†,‡] Craig L. Perkins,[§] Jason Tolentino,[†] Mohammad H. Zarghami,[†,‡] Jorge Bustamante, Jr.,[†] and Matt Law*[,†,‡]

[†]Department of Chemistry and [‡]Center for Advanced Solar Photophysics, University of California, Irvine, Irvine, California 92697, United States

[§]National Renewable Energy Laboratory, Golden, Colorado 80401, United States

Supporting Information

ABSTRACT: Thin films of colloidal semiconductor nanocrystals (NCs) are inherently metatstable materials prone to oxidative and photothermal degradation driven by their large surface-to-volume ratios and high surface energies.[1] The fabrication of practical electronic devices based on NC solids hinges on preventing oxidation, surface diffusion, ripening, sintering, and other unwanted physicochemical changes that can plague these materials. Here we use low-temperature atomic layer deposition (ALD) to infill conductive PbSe NC solids with metal oxides to produce inorganic nanocomposites in which the NCs are locked in place and protected against oxidative and photothermal damage. Infilling NC field-effect transistors and solar cells with amorphous alumina yields devices that operate with enhanced and stable performance for at least months in air. Furthermore, ALD infilling with ZnO lowers the height of the inter-NC tunnel barrier for electron transport, yielding PbSe NC films with electron mobilities of 1 $cm^2 V^{-1} s^{-1}$. Our ALD technique is a versatile means to fabricate robust NC solids for optoelectronic devices.

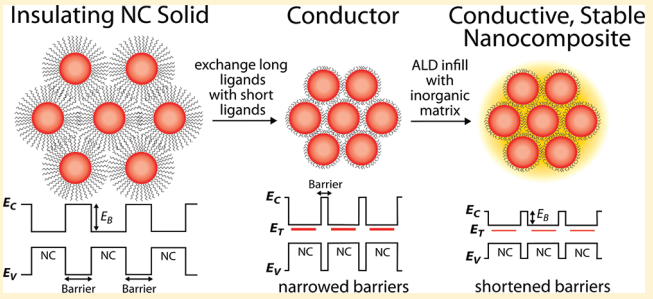

KEYWORDS: Nanocrystal, quantum dot, PbSe, atomic layer deposition, solar cell

Optoelectronic devices based on films of lead chalcogenide (PbX, X = S, Se, Te) nanocrystals (NCs) tend to degrade rapidly in air because the short-chain organic capping ligands commonly used to prepare conductive NC films provide meager protection against oxidation.[2−5] For example, exposing Schottky-type PbSe NC solar cells treated with 1,2-ethanedithiol (EDT, a common ligand for making conductive PbX NC films) to air for several minutes causes irreversible linearization of the current−voltage characteristics and loss of photovoltaic action (Supplementary Figure 1a, Supporting Information). Similarly, hydrazine-capped, n-channel PbSe NC field-effect transistors (FETs)[6,7] become p-type and significantly more conductive after one minute in air (Supplementray Figure 1b, Supporting Information). The poor oxidative stability of PbSe NCs (and of nanoscale materials more generally) is an obstacle to both practical applications and fundamental studies of charge transport, doping, and junction formation in nanoscale systems. On the other hand, this poor stability also makes PbSe NC solids an important model system for testing strategies to manufacture truly robust, functional NC materials.

Here, we overcome the instability of organic ligand-capped NCs by preparing neat films of random-packed, electronically coupled PbSe NCs using layer-by-layer dip coating[8] and then infilling the pores of these films with various *inorganic* matrices—including amorphous Al_2O_3 and crystalline ZnO—by low-temperature ALD (<80 °C). The inorganic matrix acts to suppress oxidative and photothermal degradation of the NCs and can also reduce the size of the inter-NC tunnel barriers that govern the motion of charge carriers, thereby improving carrier mobility through the films. ALD is a stepwise chemical vapor deposition method for depositing thin conformal films onto nonplanar substrates with submonolayer thickness control, and low-temperature ALD is of increasing importance for growing high-quality films on topologically complicated substrates.[9−16] ALD has been used to fill the pores of TiO_2 NC films consisting of NCs with diameters as small as 10 nm.[17] More recently, ZnO deposited by ALD at 100 °C was shown to penetrate CdSe quantum dot films and increase film conductivity and carrier mobility.[18]

Figure 1a illustrates our overall fabrication scheme and Figure 1b shows an X-ray photoelectron spectroscopy (XPS) elemental depth profile of a 330 nm thick PbSe NC film (6.1 nm NCs, E_g = 0.678 eV) infilled with alumina deposited by ALD of $Al(CH_3)_3$ and H_2O at 70 °C. The presence of aluminum and oxygen throughout the NC layer shows that alumina fills the nanoscale void network of the NC film to the surface of the substrate (indium tin oxide (ITO) coated glass in this case). The first few nanometers of alumina coat the

Received: August 19, 2011
Revised: October 5, 2011
Published: October 24, 2011

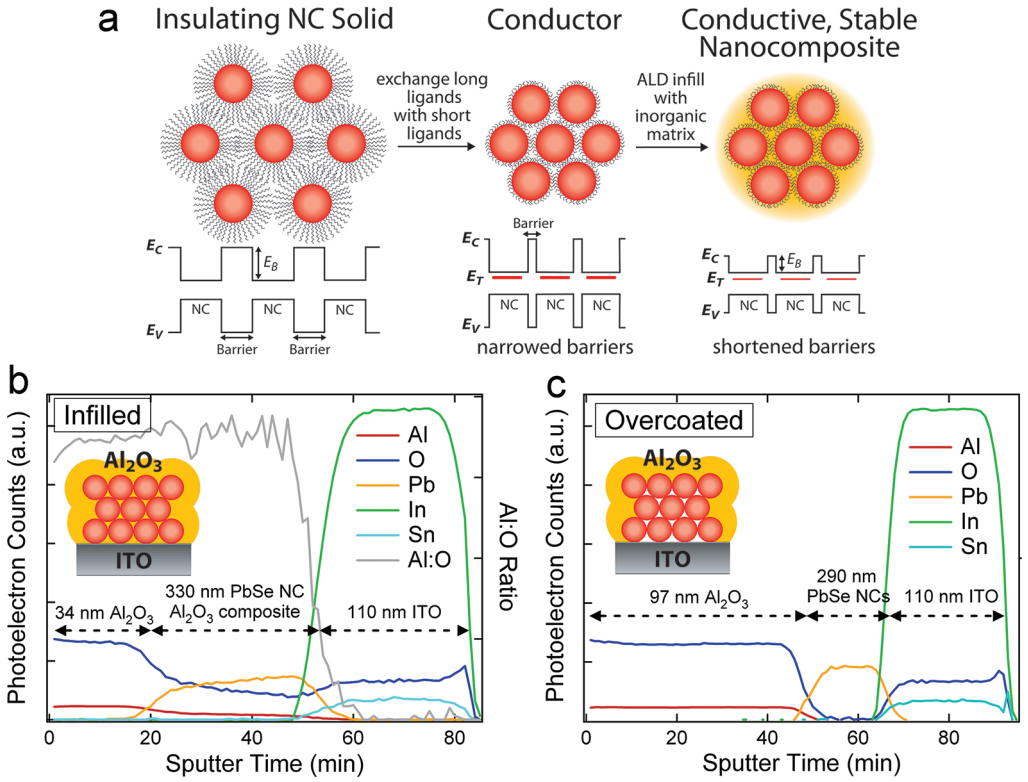

Figure 1. ALD-infilled NC solids as robust and functional granular electronic materials. (a) Conductive NC films made by ligand exchange with short-chain organic molecules are infilled with metal oxides by low-temperature ALD, creating stable inorganic nanocomposites. Organic ligand exchange reduces the inter-NC barrier width, while infilling with an appropriate inorganic material can lower the barrier height and boost carrier mobility. (b) XPS depth profile of a PbSe NC film (330 nm thick film of formic acid treated, 6.1 nm NCs on an ITO substrate) infilled with ALD alumina at 70 °C. The elemental profiles and constant Al:O ratio show that Al_2O_3 is present throughout the NC film. ALD infilling is a general process that works for many different ligands, NC sizes, and deposition temperatures, including room temperature (Supplemental Figure 2, Supporting Information). (c) XPS profile of an EDT-treated NC film overcoated (not infilled) with CVD Al_2O_3 at 70 °C in the same deposition chamber. The core levels plotted are Al 2p, O 1s, Pb $4d_{5/2}$, In $3d_{5/2}$, and Sn $3d_{5/2}$.

accessible internal surface of the film to make a three-dimensional $PbSe/Al_2O_3$ inorganic nanocomposite. Further ALD ultimately seals off the pore network and forms a capping layer of alumina on the external surface of the film. The opposite slopes of the Al and Pb data within the NC layer may indicate incomplete infilling of the available pore space, probably due to diffusion limitations and the greater chance for pores far from the film surface to be sealed off by ALD before being completely infilled. It is also possible that the NCs are more densely packed toward the base of the film. We can control whether a NC film is infilled or merely overcoated with alumina by adjusting the purge time after a water pulse: a short purge time leaves a multilayer of water on the film surface that reacts with $Al(CH_3)_3$ in a chemical vapor deposition (CVD)-like fashion to yield an oxide overlayer without substantial pore filling. Overcoated films show uniform, aluminum-free PbSe NC layers underneath the alumina coatings (Figure 1c) and serve to rule out possible sampling artifacts (such as ion-beam induced mixing) in the depth profile data of our infilled samples.

ALD infilling of complete NC field-effect transistors yields devices that are stable against oxidation. Figure 2 compares the impact of air exposure on the performance of uncoated and alumina-infilled PbSe NC FETs. Uncoated EDT-treated FETs show ambipolar conductivity when measured in an oxygen- and moisture-free (<0.1 ppm) glovebox,[8,19,20] but these devices degrade quickly in air, becoming more conductive, heavily hole doped, and nearly unresponsive to applied gate fields after only 20 s of air exposure (Figure 2a,b). Our studies of EDT-treated PbSe NC films show that oxidation is a two-stage process consisting of (i) rapid (within seconds) oxidative desorption of EDT and adsorption of O_2 and H_2O species that dope the film with holes and increases its conductivity, and (ii) slow (over months) formation of an oxide shell around each NC that gradually decreases the film conductivity (see Supplementary Figures 3−8 in the Supporting Information for details). Infilling EDT-treated NC FETs with alumina prevents such oxidation by forming a dense, conformal diffusion barrier over all accessible internal and external surfaces of a NC device. Panels c and d of Figure 2 show typical output and transfer characteristics of a NC FET before ALD treatment, after depositing 10 nm of ALD alumina at 27 °C, and after storing the infilled device in air for 34 days with periodic electrical testing. The ALD process preserves the ambipolar characteristics of the original device because the deposition temperature is low enough to avoid EDT desorption, NC ripening, sintering, and etching, and the films are not exposed to air prior to ALD infilling (our ALD chamber was built in a glovebox). In air, the infilled FETs can operate as ambipolar transistors for at least months without sign of oxidation. Electron and hole field-effect mobilities calculated from the transfer data typically double over the weeks following ALD infilling (reaching up to 0.1 and 0.03 $cm^2\ V^{-1}\ s^{-1}$, respectively), but this upward drift in mobility occurs for samples stored in both air and the glovebox and so probably reflects some (as yet unexplained)

dx.doi.org/10.1021/nl2028848 |*Nano Lett.* 2011, 11, 5349–5355

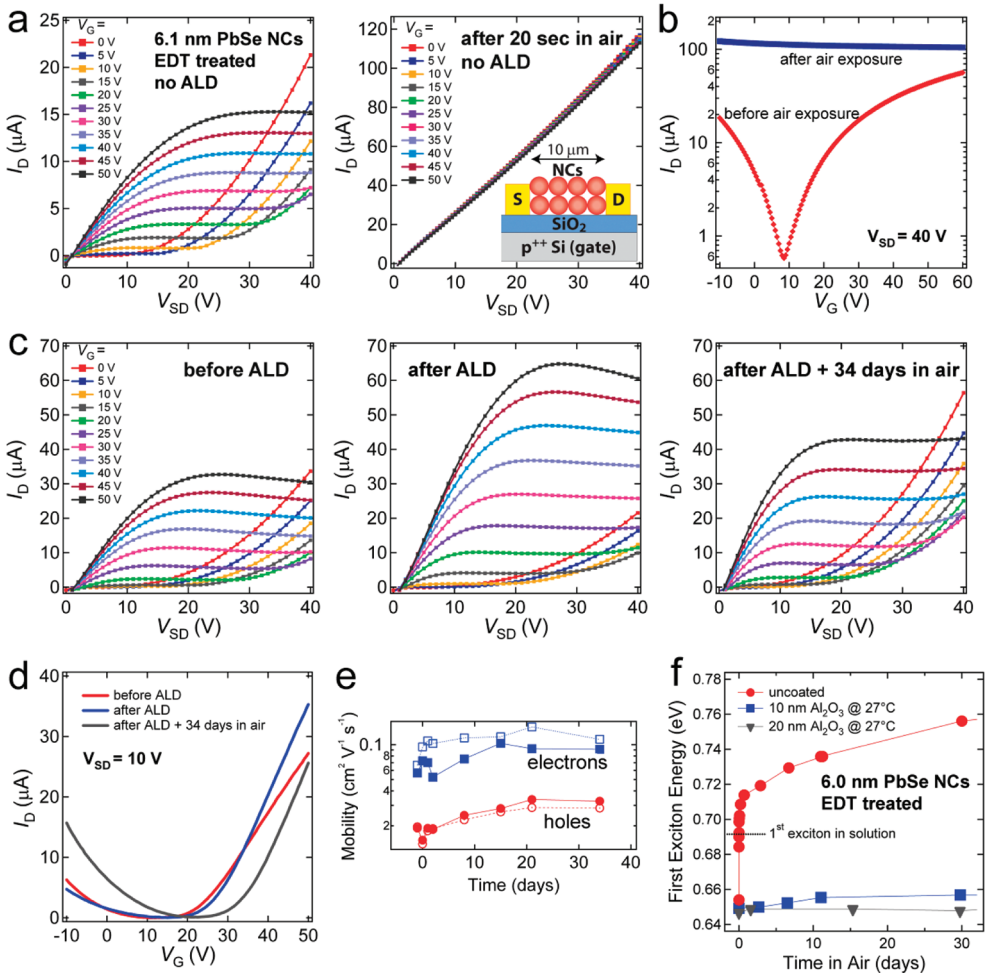

Figure 2. Oxidation behavior of uncoated and ALD-infilled NC field-effect transistors. (a) Output curves of an uncoated, EDT-treated PbSe NC FET before and after a 20 s exposure to laboratory air (6.1 nm NCs). The device, which shows ambipolar conduction before air exposure, becomes p-type with increased conductivity and very poor current modulation after air exposure. Inset is a cartoon of the device. (b) Transfer curves of the device in its pristine and oxidized states. V_{SD} = +40 V. (c) Output characteristics of a second, identically prepared NC FET measured before ALD coating, after coating with 10 nm of Al_2O_3 at 27 °C, and after exposing the ALD-treated FET to air for 34 days. (d) The corresponding transfer curves at V_{SD} = +10 V. (e) Electron and hole mobility as a function of time after ALD coating: closed symbols, a device stored in air; open symbols, an identical device stored in a glovebox. The first data point of each trace is the mobility before ALD treatment. V_{SD} = +10 V. (f) Energy of the first excitonic transition of an uncoated film and two ALD-infilled films versus time stored in air (6.0 nm NCs). Shift of the exciton to higher energy indicates oxidation of the NCs in the uncoated film; this blue shift is suppressed by the 10 nm alumina coating and eliminated by the 20 nm coating.

intrinsic aging process of the ALD-treated films rather than bona fide oxidation (Figure 2e). By itself, alumina infilling at 27 °C has little effect on the measured carrier mobility, but infilling at higher temperatures tends to increase mobility values of EDT-treated samples by up to an order of magnitude (Supplementary Figure 9, Supporting Information). We attribute the increased electron and hole mobility after alumina infilling to trap passivation rather than barrier lowering, since the effect depends on the ALD process temperature and ligand treatment.

We also monitored oxidation optically by looking for steady blueshifting of the first excitonic absorption peak, which is a typical signature of increasing electronic confinement due to the buildup of wide-band-gap oxides on the NC surface.[21,22] Whereas uncoated films show asymptotic blue shifts of 100−120 meV over the first month in air, ALD-infilled films give either very small blue shifts (<10 meV for 10 nm coatings deposited at 27 °C) or none at all (for 20 nm coatings made at 27 °C or for thinner coatings deposited at >50 °C; Figure 2f and Supplementary Figure 10 in the Supporting Information). The absence of any blue shift from the ALD infilling itself suggests that the encased NCs are not oxidized by deposition of the alumina coating. This is consistent with our XPS results showing that the NCs are not oxidized by water exposure alone (Supplementary Figure 4, Supporting Information). These results confirm that ALD infilling with alumina can inhibit NC oxidation without deleteriously affecting the electrical behavior of complete NC devices. Moreover, this ALD technique is effective for a wide range of NC sizes, capping ligands, and deposition temperatures (Supplementary Figure 10, Supporting Information), making it a general method for enhancing the stability and functionality of electronic devices built from NC solids and other classes of nanomaterials.

ALD alumina treatments can greatly improve the efficiency and stability of Schottky-type PbSe NC solar cells. Our early efforts to extend the ALD strategy to whole NC solar cells were unsuccessful because the top metal electrodes block vertical diffusion of ALD precursors into the underlying active area of the

dx.doi.org/10.1021/nl2028848 |Nano Lett. 2011, 11, 5349–5355

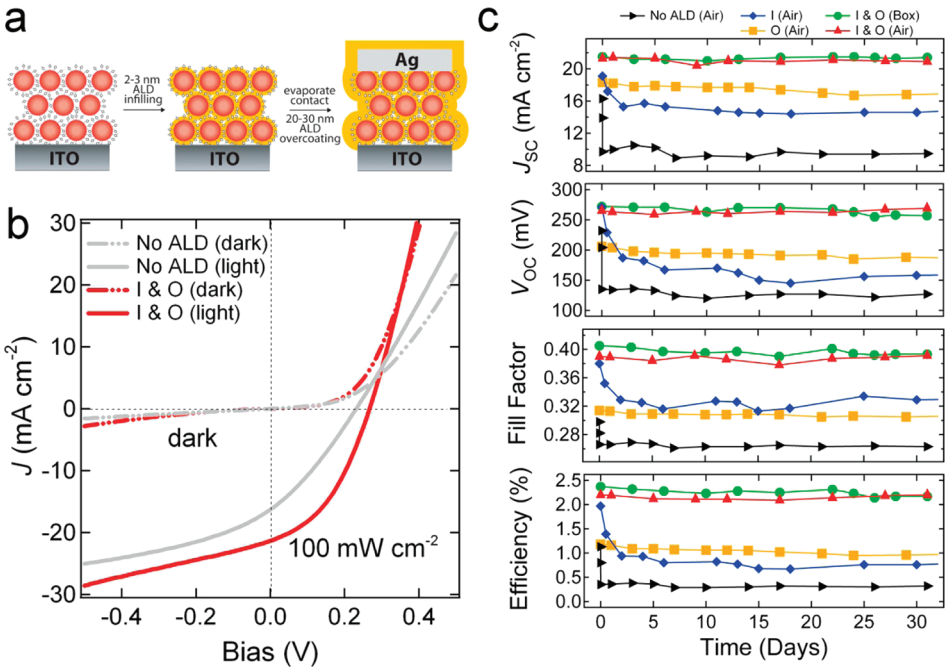

Figure 3. ALD-treated PbSe NC solar cells. (a) Cartoon of the fabrication process. (b) Representative current−voltage curves for ITO/PbSe NC/Ag Schottky solar cells with no ALD alumina treatment (gray curves) and with 3 nm of ALD infilling followed by 30 nm of ALD overcoating (red curves). The ALD treatments double the device efficiency. The thicknesses of the ITO, NC, and Ag layers are 115, 145−150, and 45−50 nm, respectively (see Supplemental Figure 11, Supporting Information). This device was measured before exposure to air. (c) Time traces of J_{SC}, V_{OC}, fill factor, and power conversion efficiency for a set of devices prepared with no ALD treatment (black triangles), 3 nm infilling and no overcoating (diamonds), 30 nm overcoating and no infilling (squares), and infilling plus overcoating (circles and red triangles). These devices were stored in the dark either in air or in a glovebox, as indicated. NC diameter = 3.7 nm. ALD temperature = 54 °C.

NC films. To overcome this problem, we developed a fabrication protocol consisting of the following steps: (1) deposit the NC film by dip coating; (2) infill the film with 2−3 nm of ALD alumina; (3) evaporate the top metal electrode; (4) overcoat the entire device with 20−30 nm of ALD alumina. These two ALD treatments have complementary functions: the infilling step creates the inorganic nanocomposite and alters the surfaces of the NCs to increase the cell conversion efficiency, while the overcoating step creates a conformal gas diffusion barrier that greatly enhances device stability.

The impact of the ALD treatments on the efficiency and stability of 1,4-benzendithiol (BDT)-treated PbSe NC Schottky cells (ITO/PbSe NCs/Ag) is illustrated in Figure 3. Devices that are both infilled (I) and overcoated (O) show significant increases in short-circuit current density (J_{SC}), open-circuit voltage (V_{OC}), and fill factor, with typically twice the conversion efficiency of identical devices prepared with no ALD treatments (e.g., from 1.1% to 2.2% for the cells in Figure 3). Furthermore, infilled and overcoated devices retain more than 95% of their performance after 1 month of storage in air, while untreated devices degrade within hours in air to ∼30% of their original efficiency (and stabilize thereafter). Control devices that are overcoated but not infilled show similarly improved stability but without improved efficiency, suggesting that alumina deposited onto complete solar cells acts primarily as a gas diffusion barrier that dramatically slows oxidative degradation. In contrast, control devices that are infilled but not overcoated show most of the efficiency enhancement but with only slightly better stability (degradation to ∼30% of initial efficiency in days instead of hours); these observations support the notion that alumina infilling improves the electronic properties of the NC film and/or the NC/metal junction but is too thin to stop oxidation. The improved efficiency probably results from a combination of carrier mobility enhancement via trap passivation and a larger built-in voltage at the NC/Ag Schottky contact, although other mechanisms may also be active and are under investigation.

It is somewhat surprising that a 2−3 nm thick alumina coating deposited on the NC film prior to evaporation of the silver electrode improves device efficiency rather than greatly increasing the series resistance and lowering J_{SC} and efficiency. This can be understood if the thin alumina films are either discontinuous, poorly resistive, or readily punched through by the evaporated metal contact. We observed that somewhat thicker alumina infilling dramatically suppressed J_{SC} and efficiency (Supplemental Figure 12, Supporting Information), while very thick (>30 nm) alumina interlayers made very resistive, nonfunctional devices. Transmission electron microscopy (TEM) images verified that our ALD infilling process yields conformal and continuous amorphous alumina films on BDT-treated PbSe NCs (Supplemental Figure 13, Supporting Information). Furthermore, planar alumina films on ITO substrates were highly resistive ($\rho > 10^{12}$ Ω cm) when measured with silver paint or evaporated gold top contacts (Supplemental Figure 14, Supporting Information). These resistivity values are in accord with previous studies of the electrical properties of thin alumina films.[23] However, we found that the through-plane resistivity of thin (<30 nm) alumina films was very low ($\rho < 10^{5}$ Ω cm) when evaporated silver contacts were used, suggesting that the evaporated silver eats through thin alumina films during the deposition process. On the basis of these observations, we believe that, at 2−3 nm, the infilling layer is thick enough to fill the interstitial volume of the NC film yet sufficiently thin to allow the evaporated silver contact to

dx.doi.org/10.1021/nl2028848 |Nano Lett. 2011, 11, 5349–5355

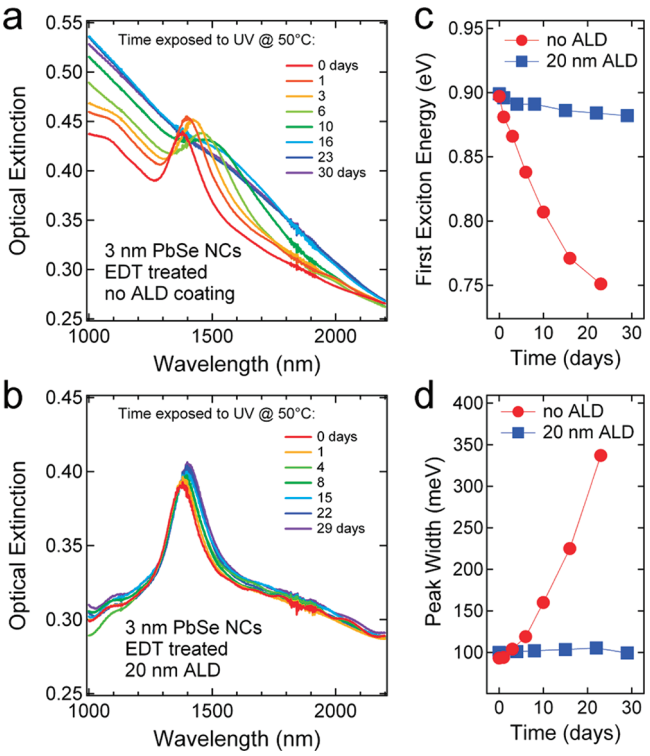

Figure 4. Arrested photothermal degradation of ALD-infilled NC films. (a) Optical absorption spectra of an uncoated, EDT-treated film of 3 nm PbSe NCs exposed to UV light (365 nm, 1.4 mW cm^{-2}) at 50 °C in a glovebox (1−5 ppm O_2 and H_2O) for 1 month. (b) Spectra of an identical film infilled with 20 nm of Al_2O_3 deposited at 27 °C. (c) Energy and (d) width of the first exciton absorption peak over time for both samples. The ALD matrix greatly suppresses UV-induced coarsening of the NCs. Film thickness: ∼150 nm.

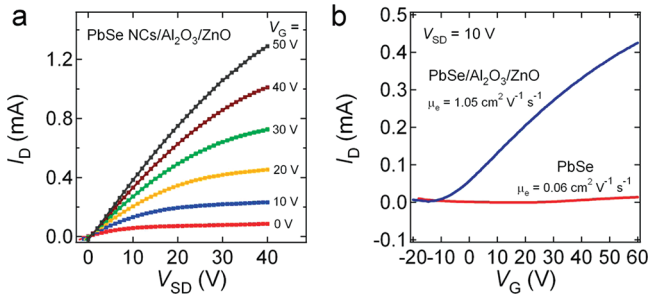

Figure 5. ZnO-infilled NC FETs with increased electron mobility. (a) Output curves for a NC FET with a channel composed of 6.1 nm PbSe NCs capped with EDT and infilled with 1 nm of alumina followed by 5 nm of ZnO at 75 °C. The FET was then overcoated with 30 nm of alumina to guarantee its air stability. (b) Plots of drain current I_D versus gate voltage V_G for the FET before and after ALD coating. See Supplemental Figure 19 (Supporting Information) for a plot of these data on log−linear axes. Channel length = 25 μm. Channel width = 1000 μm.

punch through the alumina shell that covers the topmost layer of NCs and form a good electrical contact. Presumably the NC/Ag interfacial region consists of a mixed PbSe/BDT/alumina layer containing various intermediate phases.

ALD is widely considered to be too slow a method for practical manufacturing. Although we use ALD both to infill and overcoat NC solar cells in this study, in practice the 2−3 nm infilling layer would be deposited by ALD and the much thicker gas diffusion barrier (the overcoat) could be made by a faster encapsulation technique. Because it is only 2−3 nm thick, the infilling layer can be deposited in minutes or less and is well suited to rapid, large-scale batch fabrication or roll-to-roll manufacturing.[24]

In addition to inhibiting oxidation, ALD infilling is also effective at preventing photothermal degradation of NC films. NCs are inherently metastable objects because a reduction in surface area will significantly lower their free energy.[1] As a result, NC films can sinter at temperatures far below the sintering temperature of the corresponding bulk materials. We monitored changes in the optical spectra of 150 nm thick films of 3 nm PbSe NCs exposed continuously for 1 month to moderate heat (50 °C) and UV light in a nitrogen glovebox (Figure 4). Spectra of films with no ALD infilling exhibited a dramatic red shift and broadening of the first exciton peak, indicating an increase in both the average NC diameter and the diameter distribution. Because films exposed to heat alone (no UV light) showed much smaller red shifts and broadening after the same exposure time (Supplemental Figure 15, Supporting Information), we attribute most of the spectral changes to a UV-induced coarsening process in which localized heating from the thermalization of hot excitons promotes surface diffusion and NC sintering. ALD infilling prevents such coarsening by encasing the NCs in an alumina matrix, resulting in optical spectra that change very little in response to heat and light soaking (Figure 4b). Slight red shifts *are* observed for ALD-infilled films composed of very small NCs (Figure 4c), presumably due to the presence of poorly infilled domains within the very narrow void networks of these films. ALD-infilled films of bigger NCs (diameters >5 nm) showed no appreciable red shifting or broadening after photothermal testing (Supplemental Figure 16, Supporting Information). Our results, as well as the recent demonstration of >1000 h air and light stability of 3% efficient heterojunction PbS NC devices,[25] show the excellent potential of PbX NC solar cells to achieve long-term stability. Future heat, light, and humidity soaking will establish whether ALD-infilled NC solar cells can meet the stringent stability requirements of commercial photovoltaics.

We conclude by demonstrating that ALD infilling can increase carrier mobilities in NC solids by reducing the effective height of the inter-NC transport barrier. Figure 5 shows the output and transfer characteristics of an EDT-treated PbSe NC FET infilled with 1 nm of Al_2O_3 followed by 5 nm of ZnO at 75 °C. Prior to infilling, this ambipolar device showed linear electron and hole mobilities of 0.06 and 0.02 $cm^2\ V^{-1}\ s^{-1}$, respectively. Upon infilling, the electron mobility increased by a factor of 17 to 1.05 $cm^2\ V^{-1}\ s^{-1}$, while the hole mobility approximately doubled. ZnO is expected to selectively lower the electron tunnel barrier because its conduction band lies within 0.1−0.4 V of the $1S_e$ level of large PbSe NCs at equilibrium.[26,27] Such good alignment of the ZnO and PbSe conduction band edges implies a large difference in valence band energies and a substantial barrier (>2 eV) to hole transport through the NC films. This band energy alignment explains why the electron mobility increases markedly while the hole mobility only doubles upon ZnO infilling (the latter probably as a result of trap passivation). FETs with channels composed of pure ZnO films (without NCs) had much lower conductivity and electron mobility (<0.006 $cm^2\ V^{-1}\ s^{-1}$), showing that the high electron mobility is a property of the NC composite rather than the ZnO film itself (Supplemental Figure 17, Supporting Information). XPS depth profiles verified

dx.doi.org/10.1021/nl2028848 |*Nano Lett.* 2011, 11, 5349–5355

that these thin FET films could be infilled with both alumina and ZnO (Supplemental Figure 18, Supporting Information). Inclusion of a thin alumina interlayer between ZnO and PbSe was necessary to reduce the conductivity of the FET channel to the level where it could be effectively gated. Further study is needed to better understand the internal nanoscale structure of these infilled NC films in order to more rationally tune their electronic properties. We note that Kovalenko et al. recently achieved high electron mobility values by solution-phase exchange of organic ligands with inorganic molecular chalcogenide ligands to produce all-inorganic CdSe NC solids.[28] The use of high-mobility NC composites should result in large improvements in the photocurrent and efficiency of next-generation NC solar cells.

We have demonstrated ALD infilling as a versatile method for making PbX NC-based electronic materials with enhanced performance and unprecedented oxidative and photothermal stability. The ALD coatings slow oxidation, prevent internal atomic and molecular motion, and modify inter-NC barrier heights, surface trap densities, and other electronic characteristics of NC films. The unrivaled ability of ALD to conformally coat nanostructured substrates with functional materials—including semiconductors, metals, and catalyst layers—offers many exciting opportunities to fabricate high-performance, robust nanomaterials for optoelectronics.

Methods. *Chemicals.* Lead oxide (PbO, 99.999%), selenium (99.99%), oleic acid (OA, tech. grade, 90%), diphenylphosphine (DPP, 98%), trioctylphosphine (TOP, tech. grade, >90%), 1-octadecene (ODE, 90%), 1,2-ethanedithiol (EDT, >98%), formic acid (98%), acetic acid (99.99%), anhydrous hydrazine, trimethylaluminum (97%), diethylzinc, and anhydrous solvents were purchased from Aldrich and used as received. 1,4-Benzenedithiol (BDT) was acquired from Alfa Aesar and 1,5-pentanedithiol (>98%) from Acros.

NC Synthesis. PbSe NCs were synthesized and purified using standard air-free techniques. In a typical synthesis, a solution of 1.09 g of PbO (4.9 mmol), 3.45 g of oleic acid (12.2 mmol), and 13.5 g of ODE was degassed in a three-neck flask and heated at 180 °C for 1 h to dissolve the PbO and dry the solution. Fifteen milliliters of a 1 M solution of TOP-Se containing 0.14 g of DPP (0.75 mmol) was then rapidly injected into this hot solution. The NCs were grown for preselected times (1−15 min), and the reaction was then quenched with a water bath and 20 mL of anhydrous hexane. The NCs were purified by three rounds of dispersion/precipitation in hexane/ethanol and stored in a glovebox as a powder.

NC Film Deposition. A mechanical dip coater mounted inside of a glovebox (DC Multi-4, Nima Technology) was used to prepare PbSe NC films via a layer-by-layer procedure described in detail elsewhere.[2,29] Briefly, the substrates (glass, silicon, quartz, or prepatterned FET or ITO substrates, cleaned by sonication in acetone followed by rinses in acetone and isopropanol and drying under an N_2 flow) were alternately dipped into a 2 mg mL^{-1} solution of NCs in dry hexane and then a 1 mM solution of the appropriate short-chain ligand in dry acetonitrile. In the case of the butanedithiol and pentanedithiol treatments (both nonvolatile ligands), a third beaker containing pure acetonitrile was used to rinse the films after each dip in the dithiol solution in order to remove any residue. We fabricated films with thicknesses in the range of 20−350 nm (thin for FETs, thicker for XPS, UV−Vis, and solar cell studies). This dip coating procedure results in uniform, optically smooth, and crack-free NC films.[8,29] Films of oleate-capped NCs ("untreated films") were made by spin coating a 300 mg mL^{-1} solution of NCs in octane at 600 rpm for 30 s, followed by 1200 rpm for 30 s.

Atomic Layer Deposition Infilling. Amorphous Al_2O_3 was deposited in a homemade cold-wall traveling wave ALD system within a glovebox from trimethylaluminum and water at a substrate temperature of 27−75 °C and an operating pressure of ∼0.15 Torr. Pulse and purge times were 10 ms and 90−120 s, respectively. The density of ALD alumina films made in this temperature range is reported to be 2.5−2.75 g cm^{-3}.[9] Crystalline ZnO was deposited from diethylzinc and H_2O at substrate temperatures of 27−75 °C and an operating pressure of ∼0.15 Torr using pulse and purge times of 10 ms and 20−70 s, respectively. ALD film thicknesses were determined via SEM and ellipsometry on planar silicon substrates. ZnO crystallinity at 27−75 °C was confirmed by XRD.

Field-Effect Transistor Measurements. NC films were dip coated onto degenerately doped silicon substrates that were coated with a 200 nm thick thermal SiO_2 gate oxide and patterned with source/drain electrodes (5 nm Ti/35 nm Au, 10 or 25 μm channel length, 1000 μm width). Film thicknesses of 20−35 nm (<10 NCs thick) were used. Unwanted areas of each film were removed with a swab. FET measurements were performed in a glovebox with a homemade probe station using a Keithley 2636A dual-channel SourceMeter driven by LabVIEW software. Electron and hole mobilities μ_{lin} were calculated from transfer curves acquired at positive and negative V_{SD}, respectively, according to the gradual channel approximation equation in the linear regime

$$\left.\frac{\partial I_D}{\partial V_G}\right|_{V_{SD}=\text{comstant}} = \frac{WC_{ox}V_{SD}}{L}\mu_{lin}$$

where W is the channel width, L the channel length, and C_{ox} the capacitance per unit area of the gate oxide. The mobility data reported here were reproduced at least three times.

Solar Cell Fabrication. PbSe NC films were deposited onto cleaned, patterned ITO-coated glass substrates (12 Ω/square, Colorado Concept Coatings) using layer-by-layer dip coating. After the ALD infilling step, top contacts (45−50 nm Ag) were evaporated through a shadow mask in a glovebox thermal evaporator (1×10^{-6} Torr base pressure) at a rate of 1.0 Å s^{-1}. The ALD overcoating layer was then deposited over the complete devices. Unwanted areas of each film were removed with a razor blade. This procedure yields four devices per substrate, each with an active area of 0.25 cm^2.

Characterization. Transmission electron microscopy (TEM) characterization was performed on a Philips CM 20 operating at 200 kV. Optical absorption spectra were acquired with a PerkinElmer Lambda 950 spectrophotometer operating in transmission mode. Samples were sealed within cells consisting of two mated 1.33 inch ConFlat sapphire viewports. Films mounted in these cells show negligible oxidation after months of storage in air. The cells were then opened and the films were stored in ambient laboratory air and light for the duration of the oxidation studies.

XPS was performed using a modified Physical Electronics 5600 XPS with monochromatic Al Kα radiation and a pass energy of 29 eV. The films were found to charge slightly during analysis, so spectra were aligned by placing the Pb $4f_{7/2}$ peak at the lowest observed binding energy of 137.3 eV. The cluster tool to which the XPS system is attached enables analysis of films

dx.doi.org/10.1021/nl2028848 |*Nano Lett.* 2011, 11, 5349–5355

without exposing them to air, as well as controlled exposures to pure oxygen gas (99.9999%) or pure water vapor (subjected to three freeze−pump−thaw cycles) via separate bleed valves in a side chamber.

Electrical measurements were acquired in a glovebox with a homemade probe station using a Keithley 2636A Dual-channel SourceMeter for the solar cells and a Keithley 238 SMU for the four-point samples (25 μm × 1000 μm electrodes on Pyrex wafers). All samples were measured at room temperature in ambient laboratory light. Solar cells were tested under 100 mW cm^{-2} AM1.5G simulated sunlight (Newport model 91160). The light intensity was calibrated with a pyroelectric radiometer (model Rk-5710, LaserProbe, Inc.). Photocurrents were not corrected for spectral mismatch between the solar simulator and the true AM1.5G solar spectrum.

■ ASSOCIATED CONTENT

Supporting Information. Additional figures showing $I-V$ curves, XPS depth profiles, X-ray photoelectron spectra, absorption spectra, and SEM and TEM images. This material is available free of charge via the Internet at http://pubs.acs.org.

■ AUTHOR INFORMATION

Corresponding Author
*E-mail: matt.law@uci.edu.

■ ACKNOWLEDGMENT

Y.L., M.G., and M.H.Z. acknowledge support by the Center for Advanced Solar Photophysics (CASP), an Energy Frontier Research Center funded by the U.S. Department of Energy (DOE), Office of Science, Office of Basic Energy Sciences (BES). J.B. and M.L. were supported by the Department of Energy under Award DE-SC0003904. C.L.P. was supported by the U.S. Department of Energy under Contract No. DEAC36-G028308 with the National Renewable Energy Laboratory. J.T. acknowledges support from an NSF Graduate Research Fellowship. We thank the UCI School of Physical Sciences Center for Solar Energy for facilities support.

■ REFERENCES

(1) van Huis, M. A.; et al. Low-temperature nanocrystal unification through rotations and relaxations probed by in situ transmission electron microscopy. *Nano Lett.* **2008**, *8*, 3959–3963.

(2) Luther, J. M.; et al. Schottky solar cells based on colloidal nanocrystal films. *Nano Lett.* **2008**, *8*, 3488–3492.

(3) Koleilat, G. I.; et al. Efficient, stable infrared photovoltaics based on solution-cast colloidal quantum dots. *ACS Nano* **2008**, *2*, 833–840.

(4) Tang, J.; et al. Schottky quantum dot solar cells stable in air under solar illumination. *Adv. Mater.* **2010**, *22*, 1398–1402.

(5) Zarghami, M. H.; Liu, Y.; Gibbs, M.; Gebremichael, E.; Webster, C.; Law, M. p-Type PbSe and PbS quantum dot solids prepared with short-chain acids and diacids. *ACS Nano* **2010**, *4*, 2475–2485.

(6) Talapin, D.; Murray, C. B. PbSe nanocrystal solids for n- and p-channel thin film field-effect transistors. *Science* **2005**, *310*, 86–89.

(7) Law, M.; et al. Structural, optical and electrical properties of PbSe nanocrystal solids treated thermally or with simple amines. *J. Am. Chem. Soc.* **2008**, *130*, 5974–5985.

(8) Luther, J. M.; Law, M.; Song, Q.; Beard, M. C.; Nozik, A. J. Structural, optical and electrical properties of self-assembled films of PbSe nanocrystals treated with 1,2-ethanedithiol. *ACS Nano* **2008**, *2*, 271–280.

(9) Groner, M. D.; Fabreguette, F. H.; Elam, J. W.; George, S. M. Low temperature Al_2O_3 atomic layer deposition. *Chem. Mater.* **2004**, *16*, 639–645.

(10) Luo, Y.; Slater, D.; Han, M.; Moryl, J.; Osgood, R. M. Low-temperature, chemically driven atomic-layer epitaxy: *In situ* monitored growth of CdS/ZnSe(100). *Appl. Phys. Lett.* **1997**, *71*, 3799.

(11) Knez, M.; Kadri, A.; Wege, C.; Gösele, U.; Jeske, H.; Nielsch, K. Atomic layer deposition on biological macromolecules: metal oxide coating of tobacco mosaic virus and ferritin. *Nano Lett.* **2006**, *6*, 1172–1177.

(12) Klaus, J. W.; Sneh, O.; George, S. M. Growth of SiO_2 at room temperature with the use of catalyzed sequential half-reactions. *Science* **1997**, *278*, 1934–1936.

(13) Liang, X. H.; King, D. M.; Li, P.; Weimer, A. W. Low-temperature atomic layer-deposited TiO_2 films with low photoactivity. *J. Am. Chem. Soc.* **2009**, *92*, 649–654.

(14) Meyer, J.; et al. Reliable thin film encapsulation for organic light emitting diodes grown by low-temperature atomic layer deposition. *Appl. Phys. Lett.* **2009**, *94*, 233305.

(15) Hyde, G. K.; et al. Atomic layer deposition and biocompatibility of titanium nitride nano-coatings on cellulose fiber substrates. *Biomed. Mater. (Bristol, U.K.)* **2009**, *4*, 025001.

(16) Knez, M.; Nielsch, K.; Niinisto, L. Synthesis and surface engineering of complex nanostructures by atomic layer deposition. *Adv. Mater.* **2007**, *19*, 3425–3438.

(17) Nanu, M.; Schoonman, J.; Goossens, A. Inorganic nanocomposites of n- and p-type semiconductors: A new type of three-dimensional solar cell. *Adv. Mater.* **2004**, *16*, 453–456.

(18) Pourret, A.; Guyot-Sionnest, P.; Elam, J. W. Atomic layer deposition of ZnO in quantum dot thin films. *Adv. Mater.* **2009**, *21*, 232–235.

(19) Liu, Y.; et al. Dependence of carrier mobility on nanocrystal size and ligand length in PbSe nanocrystal solids. *Nano Lett.* **2010**, *10*, 1960–1969.

(20) Leschkies, K. S.; Kang, M. S.; Aydil, E. S.; Norris, D. J. Influence of atmospheric gases on the electrical properties of PbSe quantum-dot films. *J. Phys. Chem. C* **2010**, *114*, 9988–9996.

(21) Dai, Q.; et al. Stability study of PbSe semiconductor nanocrystals over concentration, size, atmosphere, and light exposure. *Langmuir* **2009**, *25*, 12320–12324.

(22) Sykora, M.; et al. Effect of air exposure on surface properties, electronic structure, and carrier relaxation in PbSe nanocrystals. *ACS Nano* **2010**, *4*, 2021–2034.

(23) Groner, M. D.; Elam, J. W.; Fabreguette, F. H.; George, S. M. Electrical characterization of thin Al_2O_3 films grown by atomic layer deposition on silicon and various metal substrates. *Thin Solid Films* **2002**, *413*, 186–197.

(24) http://beneq.com/sites/default/files/documents/TFS%20200R%20brochure.pdf.

(25) Luther, J. M.; Gao, J.; Lloyd, M. T.; Semonin, O. E.; Beard, M. C.; Nozik, A. J. Stability assessment on a 3% bilayer PbS/ZnO quantum dot heterojunction solar cell. *Adv. Mater.* **2010**, *22*, 3704–3707.

(26) Timp, B. A.; Zhu, X.-Y. Electronic energy alignment at the PbSe quantum dots/ZnO(1010) interface. *Surf. Sci.* **2010**, *604*, 1335–1341.

(27) Choi, J. J.; Lim, Y.-F.; Santiago-Berrios, M. B.; Oh, M.; Hyun, B.-R.; Sun, L.; Bartnik, A. C.; Goedhart, A.; Malliaras, G. G.; Abruña, H. D.; Wise, F. W.; Hanrath, T. PbSe nanocrystal excitonic solar cells. *Nano Lett.* **2009**, *9*, 3749–3755.

(28) Kovalenko, M. V.; Scheele, M.; Talapin, D. V. Colloidal nanocrystals with molecular metal chalcogenide surface ligands. *Science* **2009**, *324*, 1417–1420.

(29) Law, M.; et al. Determining the internal quantum efficiency of PbSe nanocrystal solar cells with the aid of an optical model. *Nano Lett.* **2008**, *8*, 3904–3910.